Supplementary information

Salt-Bridge Structure in Solution Revealed by 2D-IR Spectroscopy

Adriana Huerta-Viga, Sérgio R. Domingos, Saeed Amirjalayer and Sander Woutersen*

Van 't Hoff Institute for Molecular Sciences (HIMS), University of Amsterdam
Science Park 904, Amsterdam, The Netherlands

Contents

1 Vibrational-exciton model for three coupled anharmonic oscillators

Here we describe the formalism to calculate the eigenstates of three coupled anharmonic oscillators, and the elements of the transition-dipole moment matrix. The basis set chosen to describe the system is that formed by the eigenstates of non-interacting harmonic oscillators $|l, m, n\rangle$, where the oscillators have l, m and n vibrational quanta, respectively. These uncoupled oscillators are used as local modes of a system of coupled oscillators. Taking the weak pump approximation implies that a maximum of two vibrational quanta are available, and the basis set is

$$\{|0\,0\,0\rangle, |1\,0\,0\rangle, |0\,1\,0\rangle, |0\,0\,1\rangle, |2\,0\,0\rangle, |0\,2\,0\rangle, |0\,0\,2\rangle, |1\,1\,0\rangle, |1\,0\,1\rangle, |0\,1\,1\rangle\}. \tag{1}$$

Taking a dipole approximation for the potential, the hamiltonian for the zero-, one- and two-exciton manifold can be calculated.[1] The zero-exciton manifold is $H^{(0)} = (0)$. The one-exciton manifold in the local basis set is given by

$$H^{(1)} = \begin{pmatrix} \epsilon_1 & \beta_{12} & \beta_{13} \\ \beta_{12} & \epsilon_2 & \beta_{23} \\ \beta_{13} & \beta_{23} & \epsilon_3 \end{pmatrix}, \tag{2}$$

where ϵ_i are the local-mode energies, and β_{ij} are the couplings between them. The two-exciton manifold is given by

$$H^{(2)} = \begin{pmatrix} 2\epsilon_1 - \Delta_1 & 0 & 0 & \sqrt{2}\beta_{12} & \sqrt{2}\beta_{13} & 0 \\ 0 & 2\epsilon_2 - \Delta_2 & 0 & \sqrt{2}\beta_{12} & 0 & \sqrt{2}\beta_{23} \\ 0 & 0 & 2\epsilon_3 - \Delta_3 & 0 & \sqrt{2}\beta_{13} & \sqrt{2}\beta_{23} \\ \sqrt{2}\beta_{12} & \sqrt{2}\beta_{12} & 0 & \epsilon_1 + \epsilon_2 & \beta_{23} & \beta_{13} \\ \sqrt{2}\beta_{13} & 0 & \sqrt{2}\beta_{13} & \beta_{23} & \epsilon_1 + \epsilon_3 & \beta_{12} \\ 0 & \sqrt{2}\beta_{23} & \sqrt{2}\beta_{23} & \beta_{13} & \beta_{12} & \epsilon_2 + \epsilon_3 \end{pmatrix}. \tag{3}$$

Note that the anharmonicities Δ_i were introduced phenomenologically. Also note that the matrix elements of the Hamiltoninan in which two excitons are changed are zero, e.g. $\langle 2\,0\,0|H|0\,1\,1\rangle = 0$, and that $\beta_{23} = \langle 1\,0\,1|H|1\,1\,0\rangle = \langle 0\,0\,1|H|0\,1\,0\rangle$. After diagonalizing this hamiltonian, states $\{|\Omega_0^{(0)}\rangle, |\Omega_j^{(1)}\rangle, |\Omega_k^{(2)}\rangle\}$ will be obtained, with $1 \leq j \leq 3$ and $4 \leq k \leq 9$. The transition-dipole moment matrix, written in the local-mode basis set is,

$$\hat{\boldsymbol{\mu}} = \left(\begin{array}{c|ccc|cccccc}
 & \boldsymbol{\mu}_1 & \boldsymbol{\mu}_2 & \boldsymbol{\mu}_3 & & & & & & \\
\hline
\boldsymbol{\mu}_1 & & & & \sqrt{2}\,\boldsymbol{\mu}_1 & 0 & 0 & \boldsymbol{\mu}_2 & \boldsymbol{\mu}_3 & 0 \\
\boldsymbol{\mu}_2 & & & & 0 & \sqrt{2}\,\boldsymbol{\mu}_2 & 0 & \boldsymbol{\mu}_1 & 0 & \boldsymbol{\mu}_3 \\
\boldsymbol{\mu}_3 & & & & 0 & 0 & \sqrt{2}\,\boldsymbol{\mu}_3 & 0 & \boldsymbol{\mu}_1 & \boldsymbol{\mu}_2 \\
\hline
 & \sqrt{2}\,\boldsymbol{\mu}_1 & 0 & 0 & & & & & & \\
 & 0 & \sqrt{2}\boldsymbol{\mu}_2 & 0 & & & & & & \\
 & 0 & 0 & \sqrt{2}\boldsymbol{\mu}_3 & & & & & & \\
 & \boldsymbol{\mu}_2 & \boldsymbol{\mu}_1 & 0 & & & & & & \\
 & \boldsymbol{\mu}_3 & 0 & \boldsymbol{\mu}_1 & & & & & & \\
 & 0 & \boldsymbol{\mu}_3 & \boldsymbol{\mu}_2 & & & & & &
\end{array}\right). \tag{4}$$

This operator needs to be written in the exciton basis set formed by the $\{|\Omega_i^{(n)}\rangle\}$ states, which is done via a similarity transformation. The elements $\boldsymbol{\mu}_{nm}$ and the $\Omega_i^{(n)}$ energies are used to calculate the linear response, which is given by

$$\alpha_{\epsilon_1,\epsilon_2}(\omega) = \sum_j \frac{|\boldsymbol{\mu}_{0j}|^2\gamma_j}{(\omega - \Omega_j^{(1)})^2 + \gamma_j^2}, \tag{5}$$

with $1 \leq j \leq 3$ and where the $\Omega_j^{(1)}$ depend parametrically on ϵ_1 and ϵ_2, and γ_j are the homogeneous linewidths of the transitions. The 2D-IR response is given by

$$\begin{aligned}
&\Delta\alpha_{\epsilon_1,\epsilon_2}(\omega_{\text{pump}}, \omega_{\text{probe}}) = \\
-\quad &\sum_i \frac{\gamma_i^2(1+\gamma_i/\Gamma)\left[p_2|\boldsymbol{\mu}_{0i}|^2|\boldsymbol{\mu}_{0i}|^2 + p_1|\boldsymbol{\mu}_{0i}|^2|\boldsymbol{\mu}_{0i}|^2\right]}{\left[(\omega_{\text{pump}} - \Omega_i^{(1)})^2 + (\gamma_i+\Gamma)^2\right]\left[(\omega_{\text{probe}} - \Omega_i^{(1)})^2 + \gamma_i^2\right]} \\
-\quad &\sum_{i,j} \frac{\gamma_i\gamma_j(1+\gamma_j/\Gamma)\left[p_2|\boldsymbol{\mu}_{0i}|^2|\boldsymbol{\mu}_{0j}|^2 + p_1(\boldsymbol{\mu}_{0i}\cdot\boldsymbol{\mu}_{0j})^2\right]}{\left[(\omega_{\text{pump}} - \Omega_i^{(1)})^2 + (\gamma_j+\Gamma)^2\right]\left[(\omega_{\text{probe}} - \Omega_j^{(1)})^2 + \gamma_i^2\right]} \\
+\quad &\sum_{i,k} \frac{\gamma_i\gamma_k(1+\gamma_i/\Gamma)\left[p_2|\boldsymbol{\mu}_{ik}|^2|\boldsymbol{\mu}_{0i}|^2 + p_1(\boldsymbol{\mu}_{ik}\cdot\boldsymbol{\mu}_{0i})^2\right]}{\left[(\omega_{\text{pump}} - \Omega_i^{(1)})^2 + (\gamma_i+\Gamma)^2\right]\left[(\omega_{\text{probe}} - (\Omega_k^{(2)} - \Omega_i^{(1)}))^2 + \gamma_k^{*2}\right]},
\end{aligned} \tag{6}$$

with $1 \leq i, j \leq 3$ and $4 \leq k \leq 9$. The first term in this equation is the contribution to the pump-probe signal due to ground-state bleaching, the second term is the stimulated emission and the third term is the excited-state absorption. γ_i^* are the homogeneous linewidth of the $|\Omega_j^{(1)}\rangle \rightarrow |\Omega_k^{(2)}\rangle$ transitions. Γ is the half-width at half-maximum of the pump spectrum. The values for p_1 and p_2 determine the polarization between pump and probe pulses of the 2D-IR signal, and they arise from the the two possible polarizations between the pump and probe fields.[2] To calculate $\Delta\alpha_{\parallel}$, the parallel-polarization signal, $p_1 = 2,\ p_2 = -1$, and $\Delta\alpha_{\perp}$, the perpendicular-polarization signal, $p_1 = 1,\ p_2 = 2$. The fact that we measure on an ensemble of molecules in different solvent surroundings is taken into account in the model. Following the central limit theorem[3], the local-state frequencies ϵ_1 and ϵ_2 are considered to have Gaussian probability distributions around central values $\bar{\epsilon}_i$, such that the linear absorption becomes

$$\alpha_{\bar{\epsilon}_1,\bar{\epsilon}_2,\bar{\epsilon}_3}(\omega) = \iiint d\epsilon_1 d\epsilon_2 d\epsilon_3 e^{(\epsilon_1-\bar{\epsilon}_1)^2/\sigma_1^2} e^{(\epsilon_2-\bar{\epsilon}_2)^2/\sigma_2^2} e^{(\epsilon_3-\bar{\epsilon}_3)^2/\sigma_3^2}\, \alpha_{\epsilon_1,\epsilon_2,\epsilon_3}(\omega), \tag{7}$$

where σ_i are the inhomogeneous line widths of the transitions, and the integrals are performed over the range $\left(\epsilon_i - \frac{3}{2}\sigma_i, \epsilon_i + \frac{3}{2}\sigma_i\right)$. The expression to obtain the 2D-IR response is analogous to that in equation 7.

We use the vibrational-exciton model to calculate the 2D-IR response of three oscillators that are involved in a salt bridge between Gdm^+ and Ac^-. The Gdm^+ modes arise from $CN_3D_6^+$ vibrations, and the Ac^- mode from a COO^- antisymmetric stretch vibration. These modes are essentially different and thus we use different values for the intensity of their transition dipole moments $|\boldsymbol{\mu}_i|$, their anharmonicities Δ_i, and homogeneous linewidths γ_i and γ_i^*. We also take different values for their inhomogeneous linewidths σ_i. The two $CN_3D_6^+$ modes show an anticorrelation behaviour, which can be detected through the elongation of the cross peaks that occurs along the antidiagonal line of the 2D plot.[4,5] To account for this anticorrelation we include in the model a Gaussian distribution for the value of the coupling β_{ij} between the two $CN_3D_6^+$ modes, which has a width σ_β that is a parameter of the fit.

2 Fit parameters

The fitting routine uses the Levenberg-Marquardt Method to minimize $\chi^2 = \sum_{i=1}^{N} \left[\frac{y_i^{\text{exp}} - y_i^{\text{calc}}}{\sigma_i}\right]^2$, where y_i^{exp} are the measured points that have standard deviations σ_i, and y_i^{calc} are the calculated values (which depend on the fitting parameters). The fits are performed simultaneously on the parallel and perpendicular 2D-IR measurements, using an independent overall scaling factor for each. The width of the pump spectrum is $\Gamma = 3.3$ cm^{-1}, which was determined experimentally and was a fixed parameter of the fits. The 2D-IR signal is a function of the angles θ_{ij} between the transition dipole moments through the dot products of equation 7. The definition of these angles is shown in Figure S1. Note that, using these definitions, $\{\theta_{12}, \theta_{13}, \theta_{23}\}$ are not orthogonal coordinates for the orientation of the $\boldsymbol{\mu}_i$, i.e. θ_{23} cannot be changed without changing θ_{12} and θ_{13}. The angle η_3 (see Figure S1) is an independent coordinate, and $\{\theta_{12}, \theta_{13}, \eta_3\}$ were free parameters of the fit. θ_{23} was calculated afterwards via

$$\theta_{23} = \cos^{-1}\left[\sin\theta_{12}\sin\theta_{13}\cos\eta_3 + \cos\theta_{12}\cos\theta_{13}\right]. \tag{8}$$

The parameters obtained from the fit are shown in Table S1. A rule of thumb for a good fit is that the reduced chi square $\chi_r^2 = \frac{\chi^2}{N-M}$ should have a value $\sim$1 (N is the number of observation points and M the number of parameters).[6] However, the model we use is not linear in the parameters and we make several simplifications, so it is to be expected that $\chi_r^2 > 1$. Nonetheless, we find that the fits reproduce the measurements very well, despite the χ_r^2 being significantly

Table S1: Fit parameters for the $Gdm^+ \cdots Ac^-$ dimer. For each oscillator the parameters are: local-mode absorption frequency ϵ; anharmonicity Δ; homogeneous dephasing for the $|0\rangle \rightarrow |1\rangle$ transition γ_{01}, and for the $|1\rangle \rightarrow |2\rangle$ transition γ_{12}; inhomogeneous width σ; coupling between transition dipole moments β; width of the distribution of couplings σ_β; angle between transition dipole moments θ. All parameters are given in cm^{-1} and the angle in degrees. χ_r^2 is 41.

Gdm^+_{HF}		Gdm^+_{LF}		Ac^-	
ϵ	1602	ϵ	1586	ϵ	1560
Δ	4	Δ	8	Δ	14
γ_{01}	6	γ_{01}	5	γ_{01}	7
γ_{12}	7	γ_{12}	6	γ_{12}	5
σ	13	σ	22	σ	15
η_3	55				

Gdm^+_{HF}-Gdm^+_{LF}		Gdm^+_{HF}-Ac^-		Gdm^+_{LF}-Ac^-	
θ_{23}	105 ± 25 °	θ_{13}	$180° \pm 15$	θ_{12}	$75° \pm 10$
β_{23}	-8 ± 2	β_{13}	-11 ± 3	β_{12}	8 ± 3
σ_β	12				

larger than 1. The outcome of a χ^2-minimization routine is the covariance matrix, which is related to the confidence limits of the fitted parameters, but the values of χ_r^2 that we obtained are too large to follow this procedure (the resulting uncertainties are unrealistically small). Therefore, to obtain an estimate for the confidence limits in the values of β_{ij} and θ_{ij} we changed the parameter until the value for χ_r^2 was at least 50% larger. These confidence limits are listed in Table S1. The result of our fit shows that $\boldsymbol{\mu}_1$ and $\boldsymbol{\mu}_3$ are approximately antiparallel, and from equation 8, $\theta_{23} \approx 180 - \theta_{12}$, which is valid for all values of η_3. Therefore, for this geometry of transition dipole moments changing η_3 does not result in a significant increase of χ_r^2. We estimated confidence limits for θ_{23} using equation 8 with the confidence limits of θ_{12} and θ_{13}, and the full range of possible values of η_3.

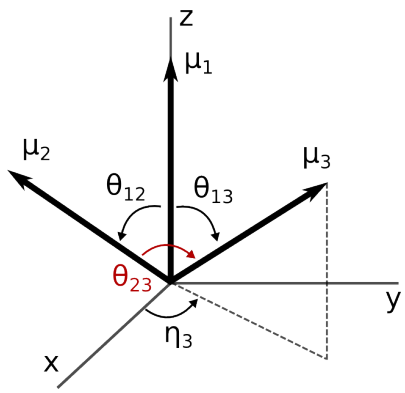

Figure S1: Definition of the angles between the transition-dipole moments θ_{ij} in the reference frame used for the fit.

3 *Ab-initio* calculations

It has been shown before that Gdm^+ has a degenerate mode at ~1600 cm^{-1} due to the CN_3 and NH_2 scissors motion.[7] In Figure S2 we show the frequencies and intensities for the vibrational modes involved in the $Gdm^+ \cdots Ac^-$salt bridge, obtained from a calculation using Gaussian03[8] at the MP2/6-311+G(d) level of theory (the optimized geometry is shown in Figure 1A of the manuscript). The lowest frequency mode in the spectrum of Figure S2 corresponds mainly to the COO^- antisymmetric stretch vibration of Ac^-, and the other two modes arise mainly from CN_3D_6 vibrations of Gdm^+. There is a high degree of mixing between the COO^- mode and both of the CN_3D_6 modes. The observed frequency splitting between these two modes upon salt bridge formation is in agreement with our measurements in DMSO, shown in Figure 1B of the manuscript.

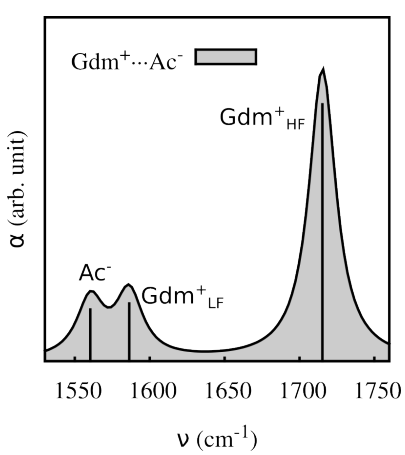

Figure S2: Frequencies and relative intensities of the vibrational modes of Gdm^+ and Ac^- obtained from the MP2 calculation of the structure shown in Figure 1 in the manuscript.

4 Sample Preparation

Guanidine·Ac (>98% purity), guanidine·HCl (>98% purity), methylguanidine·HCl (>98% purity), and tetrabutylammonium acetate (>97% purity) were purchased from Sigma-Aldrich and used without further purification. Hydrogen-deuterium exchange of the carboxyl and guanidinium groups groups of these molecules was achieved by evaporating the compounds from excess D_2O. Measurements were performed using a 400 mM concentration solution in dimethylsulfoxide (DMSO) of all compounds, at room temperature (23°C). These conditions allow more than 90% dimer formation.[9] Droplets of the solutions are placed between CaF_2 windows (2 mm thick), separated by a Teflon spacer of 10μm for the 2D-IR measurements and 25μm for the FTIR measurements.

5 Additional Data

We use a thin piece of InAs to to measure a pump-probe cross-correlation to determine the intensity envelope of the pump pulses, which is approximately a single-sided exponential with a FWHM of 800 fs. In Figure S3 we show the pump-probe cross-correlation and the resulting dynamics of a representative diagonal and cross peak. Our measurements are done at 1.5 ps delay, at which the pump pulse intensity has almost vanished.

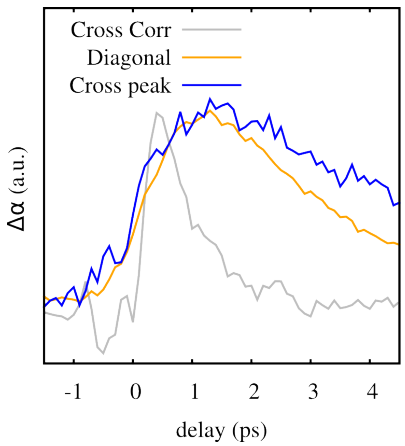

Figure S3: Cross correlation of the pump and probe pulses (gray), determined by 2-photon absorption in InAs; intensity of the induced absorption-diagonal band for when $\nu_{\mathrm{pump}} = \nu_{\mathrm{Arg_{HF}}}$ (yellow); Intensity of the induced absorption of the $\mathrm{Arg_{LF}}$ cross peak (blue).

The frequency splitting between the two CN_3H_6 modes of Gdm^+, which are centered at $\sim$1660 cm^{-1} in DMSO, is not detectable in the linear spectrum. However, a significant frequency splitting between the Gdm^+ modes is detected upon salt bridge formation with Ac^-, as seen in Figure S4.

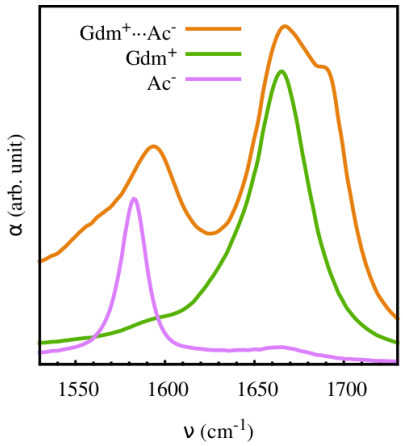

Figure S4: FTIR spectra of the non-deuterated $Gdm^+ \cdots Ac^-$ dimer, Gdm^+ and Ac^- in DMSO (solvent subtracted).

References

[1] P. Hamm and M. Zanni, *Concepts and Methods of 2D Infrared Spectroscopy*, Cambridge University Press, 1st edn, 2011.

[2] S. Mukamel, *Principles of Nonlinear Optical Spectroscopy*, Oxford University Press, 1995.

[3] R. Kubo and N. Hashitsume, *Statistical Physics II: Nonequilibrium Statistical Mechanics*, Springer, Berlin, 1985.

[4] N. Demirdöven, M. Khalil, O. Golonzka and A. Tokmakoff, *J. Phys. Chem. A*, 2001, **105**, 8025–8030.

[5] A. Ishizaki and Y. Tanimura, *J. Phys. Chem. A*, 2007, **111**, 9269–76.

[6] W. H. Press, S. A. Teukolsky, W. T. Vetterling and B. P. Flannery, *Numerical Recipes in C: The art of Scientific Computing*, Chapter 15, Cambridge University Press, 2nd edn.

[7] A. L. Magalhaes and J. A. N. F. Gomes, *Int. J. Quantum Chem.*, 1997, **61**, 725–739.

[8] M. J. Frisch and et al, *Gaussian 03, Revision C.02*, Gaussian, Inc., Wallingford, CT, 2004.

[9] B. Linton and A. D. Hamilton, *Tetrahedron*, 1999, **55**, 6027–6038.